Characterization of nighttime formation of particulate organic nitrates based on high-resolution aerosol mass spectrometry in an urban atmosphere in China

Kuangyou Yu[1,2,*], Qiao Zhu[1,*], Ke Du[2], Xiao-Feng Huang[1]

[1]Key Laboratory for Urban Habitat Environmental Science and Technology, School of Environment and Energy, Peking University Shenzhen Graduate School, Shenzhen, 518055, China.

[2]Department of Mechanical and Manufacturing Engineering, University of Calgary, Calgary, Canada.

* Authors have equal contribution.

Abstract. Organic nitrates are important atmospheric species that significantly affect the cycling of NOx and ozone production. However, characterization of particulate organic nitrates and their sources in polluted atmosphere is a big challenge and has not been comprehensively studied in Asia. In this study, an Aerodyne high-resolution time-of-flight aerosol mass spectrometer (HR-ToF-AMS) was deployed at an urban site in China from 2015 to 2016 to characterize particulate organic nitrates in total nitrates with high time resolution. Based on the cross validation of two different data processing methods, organic nitrates were effectively quantified to contribute a notable fraction of organic aerosol (OA): 9-21% in spring, 11-25% in summer, 9-20% in autumn, while very small fraction in winter. The good correlation between organic nitrates and fresh secondary organic aerosol (SOA) at night as well as the diurnal trend of size distribution of organic nitrates indicated a key role of nighttime secondary formation in Shenzhen, which is consistent with that reported in the US and Europe. The size distribution of organic nitrates also implied that organic nitrates were mainly a local product and could experience substantial loss during air mass transport. Furthermore, theoretical calculations of nighttime SOA production of NO_3 reactions with volatile organic compounds (VOCs) measured during the spring campaign were performed, resulting in three biogenic VOCs (α-pinene, limonene, and camphene) and one anthropogenic VOC (styrene) identified as the possible key VOC precursors for particulate organic nitrates. The comparison with similar studies in the literature implied that nighttime particulate organic nitrates formation is highly relevant with NOx levels. This study proposes that unlike the documented cases in the United States and Europe, modeling nighttime particulate organic nitrate formation in China should incorporate not only biogenic VOCs but also anthropogenic VOCs with high SOA yield for urban air pollution, which needs the support of relevant smog chamber studies in the future.

Correspondence to: X.-F. Huang (huangxf@pku.edu.cn)

1. Introduction

Organic nitrates (ON) in aerosols have an important impact on the fate of NO_X and ozone production (Lelieveld et al., 2016), which can be formed in a minor channel of the reaction between peroxy radicals and NO (R1 and R2) (usually, an increased fraction of this reaction leads to the formation of alkoxy radicals and NO_2 (R3)) or via the NO_3-induced oxidation of unsaturated hydrocarbons (R4). Even though some recent studies have suggested that the formation of organic nitrates from peroxy radicals and NO may play a larger role than previously recognized (Teng et al., 2015, 2017), yields of organic nitrates via NO_3 reacting with alkenes are generally much higher (Fry et al., 2009; Ayres et al., 2015; Boyd et al.,2015,2017).

$$\mathrm{RH} + \mathrm{OH} + O_2 \rightarrow RO_2 + H_2O \quad (R1)$$

$$\mathrm{R}O_2 + \mathrm{NO} \rightarrow RONO_2 \quad (R2)$$

$$\mathrm{R}O_2 + \mathrm{NO} \rightarrow RO + NO_2 \quad (R3)$$

$$\mathrm{R} = R' + \mathrm{N}O_3 \rightarrow R(ONO_2)\ R' \quad (R4)$$

Several methods have been developed to directly measure total organic nitrates (gas + particle) in the real atmosphere. For example, Rollins et al.(2012) used a thermal-dissociation laser-induced fluorescence technique (TD-LIF) to observe organic nitrates in the United States; Sobanski et al. (2017) measured organic nitrates in Germany using the thermal dissociation cavity ring-down spectroscopy (TD-CRDS). Field and laboratory studies around the world indicated that particulate organic nitrates could contribute a large portion of secondary organic aerosol (SOA) (Rollins et al., 2012; Xu et al., 2015a; Fry et al., 2013; Ayres et al., 2015; Boyd et al., 2015; Lee et al., 2016). Recently, researchers have proposed some estimation methods for particle-phase organic nitrates based on aerosol mass spectrometry (AMS) with high time resolution (Farmer et al., 2010; Hao et al., 2014; Xu et al., 2015a, 2015b). Ng et al. (2017) reviewed the nitrate radical chemistry and the abundance of particulate organic nitrates in the United States and Europe, and further concluded that particulate organic nitrates are formed substantially via NO_3+BVOC chemistry, which plays an important role in SOA formation. Unfortunately, relevant Chinese datasets are scarce yet and not included in this review. This was because (1) the contributions of organic nitrates in SOA and total nitrates in Chinese atmosphere remain poorly understood; (2) the anthropogenic and biogenic precursor emissions in China are significantly different from those in the United States and Europe, and thus cannot be easily estimated. To our best knowledge, few studies have investigated the concentrations and formation pathways of particulate organic nitrates in China. Xu et al. (2017) estimated the mass concentration of organic nitrogen in Beijing using AMS, but in this study they ignored the contribution of NO_X^+ family, which are the major fragments of organic nitrates.

Shenzhen is a megacity of China in a subtropical region, where NOx involved photochemical reactions are very active, given considerable biogenic and anthropogenic VOC emissions (Zhang et al., 2008). To assess the evolution of particulate organic nitrates in a polluted urban atmosphere, we deployed an Aerodyne high-resolution time-of-flight aerosol mass spectrometer (HR-ToF-AMS) and other instruments in Shenzhen from 2015 to 2016 in this study. Organic nitrates and their contributions to OA in different seasons were estimated by different methods using the HR-ToF-AMS datasets, based on which, the secondary formation pathway of particulate organic nitrates in Shenzhen was further explored.

2. Experiment methods

2.1 Sampling site and period

The sampling site (22.6°N, 113.9°E) was on the roof (20 m above ground) of an academic building on the campus of Peking University Shenzhen Graduate School (PKUSZ), which is located in the western urban area in Shenzhen (Figure 1). This site is mostly surrounded by subtropical plants without significant anthropogenic emission sources nearby, except a local road that is ~100 m from the site. In this study, we used the statistical data from the Meteorological Bureau of Shenzhen Municipality (http://www.szmb.gov.cn/site/szmb/Esztq/index.html) as the reference data to determine the sampling periods for four different seasons during 2015-2016, as shown in Table 1.

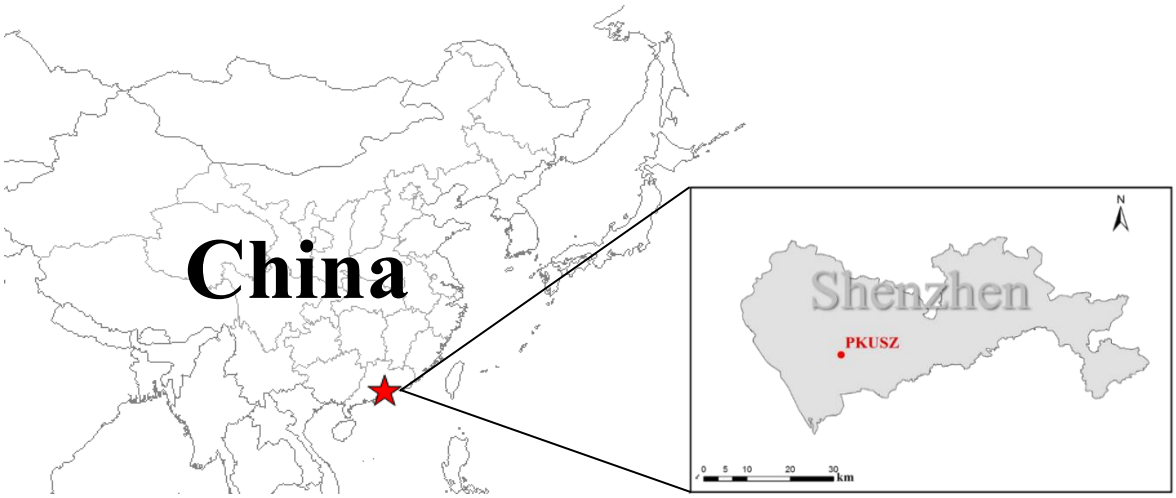

Figure 1. The location of the sampling site.

Table 1. Meteorological conditions, PM_1 species concentrations and relevant parameters for different sampling periods in Shenzhen.

	Sampling period	4.1-4.30, 2016	8.1-8.31, 2015	11.4-11.30, 2015	1.21-2.3, 2016
		Spring	Summer	Autumn	Winter
Meteorology	T (˚C)	24.5±2.5	29.0±3.0	23.6±3.7	10.7±4.7
	RH (%)	78.0±12.7	71.2±17.5	68.2±15.8	75.4±18.7
	WS (m s^{-1})	1.4±0.8	1.0±0.7	1.2±0.7	1.5±0.8
Species	Org	4.3±3.2	10.0±6.9	7.8±5.9	5.1±3.5
	SO_4^{2-}	3.2±1.8	5.8±3.3	2.3±1.5	1.9±1.2
	Total NO_3^-	0.96±1.4	0.91±0.90	1.3±1.4	1.6±1.0

(μg m^{-3})	NH_4^+	1.4±0.8	2.0±1.1	1.1±0.8	1.2±0.6
	Cl^-	0.14±0.19	0.03±0.05	0.22±0.36	0.64±0.85
	BC	1.9±2.1	2.4±1.6	3.5±2.6	2.4±1.5
	Total	12.0±8.9	15.1±13.8	11.8±9.5	12.2±7.2
ON relevant parameters	R_{NH4NO3}	2.80	3.20	3.32	3.48
	R_{obs}	3.74	6.14	4.30	3.55
	Fraction of positive numbers of R_{obs}- R_{NH4NO3}	99%	99%	84%	47%

2.2 Instrumentation

2.2.1 High Resolution Time-of-Flight Aerosol Mass Spectrometer

During the sampling periods, chemical composition of non-refractory PM_1 was measured by an Aerodyne HR-ToF-AMS, and detailed descriptions of this instrument are given in the literature (DeCarlo et al., 2006; Canagaratna et al., 2007). The setup and operation of the HR-ToF-AMS can be found in our previous publications (Huang et al., 2010, 2012; Zhu et al.,2016). To remove coarse particles, a $PM_{2.5}$ cyclone inlet was installed before the sampling copper tube with a flow rate of 10 l min^{-1}. Before entering the AMS, the sampled air was dried by a nafion dryer (MD-070-12S-4, Perma Pure Inc.) to eliminate the potential influence of relative humidity on particle collection (Matthew et al., 2008). The ionization efficiency (IE) calibrations were performed using pure ammonium nitrate every two weeks. The relative ionization efficiencies (RIEs) used in this study were 1.2 for sulfate, 1.1 for nitrate, 1.3 for chloride, 1.4 for organics and 4.0 for ammonium, respectively (Jimenez et al., 2003). Composition-dependent collection efficiencies (CEs) were applied to the data according to the method in Middlebrook et al. (2012). The instrument was operated at two ion optical modes with a cycle of 4 min, including 2 min for the mass-sensitive V-mode and 2 min for the high mass resolution W-mode. The HR-ToF-AMS data analysis was performed using the software SQUIRREL (version 1.57) and PIKA (version 1.16) written in Igor Pro 6.37 (Wave Metrics Inc.) (http://cires1.colorado.edu/jimenezgroup/ToFAMSResources/ToFSoftware / index.html).

2.2.2 Other co-located instruments

In addition to the HR-ToF-AMS, other relevant instruments were deployed at the same sampling site. An aethalometer (AE-31, Magee) was used for measurement of refractory black carbon (BC) with a resolution of 5 min. An SMPS system (3775 CPC and 3080 DMA, TSI Inc.) was used to obtain the particle number size distribution in 15–615 nm (mobility diameter) with a time resolution of 5 min. Ozone and NO_X were measured by a 49i ozone analyzer and a 42i nitrogen oxide analyzer (Thermo Scientific), respectively. In the spring campaign, ambient VOC concentrations were also measured using an on-line VOC monitoring system (TH-300B, Tianhong Corp.), including an ultralow-temperature preconcentration cold trap and an

automated in-situ gas chromatograph (Agilent 7820A) equipped with a mass spectrometer (Agilent 5977E). The system had both a flame ionization detector (FID) gas channel for C2–C5 hydrocarbons and a mass spectrometer (MS) gas channel for C5–C12 hydrocarbons, halohydrocarbons and oxygenated VOCs. A complete working cycle of the system was one hour and included five steps: sample collection, freeze-trapping, thermal desorption, GC-FID/MS analysis, heating, and anti-blowing purification. The sample collection time was 5 min. The sampling flow speed was 60 ml min^{-1}. The anti-blowing flow speed was 200 ml min^{-1}. The calibration of over 100 VOCs was performed using mixed standard gas before and after the campaign. Detection limits for most compounds were near 5 pptv. More description of this instrument can be found in Wang et al. (2014).

2.3 Organic nitrates estimation methods

In this study, we used two independent methods to estimate particulate organic nitrates based on the AMS data, following the approaches in Xu et al. (2015b). The first method is based on the NO^+/NO_2^+ ratio (NO_X^+ ratio) in the HR-AMS spectrum. Due to the very different NO_X^+ ratios of organic nitrates and inorganic nitrate (i.e., R_{ON} and R_{NH4NO3}, respectively) (Farmer et al., 2010; Boyd et al., 2015; Fry et al., 2008; Bruns et al., 2010), the NO_2^+ and NO^+ concentrations of organic nitrates ($NO_{2,ON}$ and NO_{ON}) can be quantified with the HR-AMS data via Eqs. (1) and (2), respectively (Farmer et al., 2010):

$$NO_2^+{}_{,ON} = \frac{NO_2^+{}_{,obs} \times (R_{obs} - R_{NH4NO3})}{R_{ON} - R_{NH4NO3}} \quad (1)$$

$$NO^+{}_{ON} = R_{ON} \times NO_{2,ON} \quad (2)$$

where R_{obs} is the NO_X^+ ratio from the observation. The value of R_{ON} is difficult to determine because it varies between instruments and precursor VOCs. However, R_{NH4NO3} was determined by IE calibration using pure NH_4NO_3 every two weeks for each campaign and the results showed stable values: In spring, the average R_{NH4NO3} was 2.66 for the first IE calibration and 2.94 for the second one; in summer, the average R_{NH4NO} was 3.05 and 3.34 for the first and second IE calibrations, respectively; in autumn, the average R_{NH4NO3} was 3.33 and 3.31 for the first and second IE calibrations, respectively; in winter, the average R_{NH4NO3} was 3.45 and 3.51 for the first and second IE calibrations, respectively. We adopted the R_{ON}/R_{NH4NO3} estimation range (from 2.08 to 3.99) for variation of precursor VOCs in the literature to determine R_{ON} (Farmer et al., 2010; Boyd et al., 2015; Bruns et al., 2010; Sato et al., 2010; Xu et al., 2015b), and thus two R_{ON} values were calculated for each season to provide the upper bound ($NO_{3\_org\_ratio\_1}$) and lower bound ($NO_{3\_org\_ratio\_2}$) of $NO_{3,org}$ mass concentration.

The second method is based on the traditional positive matrix factorization (PMF) analysis of HR organic mass spectra, which resolves different organic factors (Zhang et al., 2011; Ng et al., 2010; Huang et al., 2013). Combined with NO^+ and NO_2^+ ions, the same analysis of HR organic mass spectra was performed to separate NO+ and NO2+ ions into different organic factors and an inorganic nitrate factor (Hao et al., 2014; Xu et al., 2015b). The PMF analysis procedures in this study can be found in our previous publications (Huang et al., 2010; Zhu et al., 2016; He et al., 2011), resulting in three organic factors and one inorganic factor in spring, summer and autumn: a hydrocarbon-like OA (HOA) characterized by $C_nH_{2n+1}^+$ and $C_nH_{2n-1}^+$ and O/C of 0.11 to 0.18, a less-oxidized oxygenated OA (LO-OOA) characterized by $C_xH_yO_z^+$ especially $C_2H_3O^+$ and O/C of 0.28 to 0.70, a more-oxidized oxygenated OA (MO-OOA) also characterized by $C_xH_yO_z^+$ especially CO_2^+ and O/C of 0.78 to 1.24,

and a nitrate inorganic aerosol (NIA) characterized by overwhelming NO^+ and NO_2^+, as indicated in Fig S6. According to the diagnostic plots of the PMF analysis shown in Figure S2 to S4, the same organic factors as those in the traditional PMF analysis of only organic mass spectra were obtained. The NO^+ and NO_2^+ ions were distributed among different OA factors and the NIA factor; thus the concentrations of nitrate functionality (NO_{org}^+ and $NO_{2,org}^+$) in organic nitrates ($NO_{3,\,org}$) are equal to the sum of NO_2^+ and NO^+ via Eqs. (3) and (4), respectively (Xu et al., 2015b):

$$NO_{2,org}^+ = \sum([OA\ factor]_i \times f_{NO2,i}) \quad (3)$$

$$NO_{org}^+ = \sum([OA\ factor]_i \times f_{NO,i}) \quad (4)$$

where $[OA\ factor]_i$ represents the mass concentration of OA factor i, and $f_{NO2,i}$ and $f_{NO,i}$ represent the mass fractions of NO_2^+ and NO^+, respectively.

It should be noted that the 4-factor solution seemed to have a "mixed factor" problem to some extent (Zhu et al., 2018). For example, HOA mixed with COA (clear $C_3H_3O^+$ in m/z 55 for spring, summer and autumn) (Mohr et al., 2012), and BBOA mixed with LO-OOA (clear m/z 60 and 73 signals in LO-OOA in autumn) (Cubison et al., 2011). However, running PMF with more factors would produce unexplained factors but less influence on the apportionment of NO^+ and NO_2^+ ions between organic nitrates and inorganic nitrate (Table S1). In addition, the standard deviations of NO^+ and NO_2^+ ions in the OA factors across different FPEAK values (from −1.0 to 1.0) were very small (Table S2). Therefore, the 4-factor solution was used for quantifying organic nitrates in spring, summer and autumn.

3. Results and discussion

3.1 Organic nitrates estimation

Table 2 shows the concentrations of nitrate functionality in organic nitrates (i.e., $NO_{3,\,org}$), estimated by both the NO^+/NO_2^+ ratio method and PMF method, as well as their contributions to the total measured nitrate. It should be noted that the small difference between the average R_{obs} and R_{NH4NO3} in winter leads to a large portion of negative data using the NO^+/NO_2^+ ratio method (Table 1). The result from the PMF method shows that the contribution of organic nitrates in total nitrates is only 4.2% in winter (Figure S6), suggesting a negligible contribution of organic nitrates. Thus, we will only discuss organic nitrate estimation results in spring, summer and autumn. The analytical outcomes by the NO^+/NO_2^+ ratio method and by the PMF method consistently suggest that organic nitrates had the highest ambient concentration (0.34-0.53 μg m^{-3}) and proportion in total nitrates (41-64%) in summer among the different seasons. This finding agrees with the finding in (Ng et al., 2017) and it implies a seasonal trend in comparison with that of total nitrates in Table 1. Assuming the average molecular weight of organic nitrates of 200 to 300 g mol^{-1} (Rollins et al., 2012), we found that organic nitrates contributed 9-21% to OA in spring, 11-25% in summer, and 9-20% in autumn.

In the PMF method, the mass fractions of organic nitrates in HOA, LO-OOA and MO-OOA were 31%, 49% and 20%, respectively, in spring; 28%, 52% and 20%, respectively, in summer; 30%, 46% and 24%, respectively, in autumn. The major

fraction of organic nitrates occurring in LO-OOA for the three seasons implied that organic nitrates were mostly related to fresher secondary OA formation. The NIA factors in all seasons were dominated by but are not limited to NO^+ and NO_2^+. Some organic fragments, such as CO_2^+ and $C_2H_3O^+$, are also part of these factors, which agreed with the findings in the literature (Hao et al., 2014; Xu et al., 2015b; Sun et al., 2012). This indicated the potential interference of organics in the NIA factor. It is also worth to be noted that the NO^+/NO_2^+ ratios in NIA (2.93 for spring, 3.53 for summer and 3.54 for autumn) were higher than that for pure NH_4NO_3 (Table 1), indicating an underestimation of $NO_{3.org}$ concentration by the PMF method. This finding may also explain the reason that the concentration of $NO_{3.org}$ estimated using the PMF method was always close to the lower estimation bound of $NO_{3.org}$ concentration estimated using the NO^+/NO_2^+ ratio method in each season (Table 2).

Table 2. Summary of organic nitrates estimations using the NO^+/NO_2^+ ratio method and the PMF method

Sampling period	NO^+/NO_2^+ ratio method				PMF method	
	$NO_{3,org}$ (μg m^{-3})[a]		$NO_{3,org}/NO_3$		$NO_{3,org}$ (μg m^{-3})[b]	$NO_{3,org}/NO_3$
	lower	upper	lower	upper		
Spring	0.12	0.19	13%	21%	0.12	12%
Summer	0.34	0.53	41%	64%	0.39	43%
Autumn	0.21	0.33	16%	25%	0.21	16%
Winter	/	/	/	/	0.07	4.2%

[a] $NO_{3,\ org}$ for upper bound is denoted as $NO_{3\_org\_ratio\_1}$, and $NO_{3,\ org}$ for lower bound is denoted as $NO_{3\_org\_ratio\_2}$.

[b] $NO_{3,\ org}$ estimated using the PMF method is denoted as $NO_{3\_org\_PMF}$.

To further verify the reliability of the estimated results of organic nitrates, the $NO_{3,\ org}$ concentration time series calculated by the two methods in each season are shown in Figure 2a. The computed correlation coefficients (R) are good (0.82 for spring, 0.82 for summer and 0.77 for autumn), indicating that similar results were achieved. The inorganic nitrate (NO_{3_inorg*}) obtained by subtracting $NO_{3\_org\_ratio\_1}$ from total measured nitrates also correlated well with the inorganic nitrate estimated using the PMF method (R=0.92 for spring, 0.87 for summer and 0.86 for autumn). ,. While they were distinctive from those of inorganic nitrate (Figure 2b), which indicates that organic nitrates had been well separated from inorganic nitrate in this study, the diurnal trends of organic nitrates obtained by the two methods were similar in each season, with lower concentrations in the daytime and higher concentrations at night.

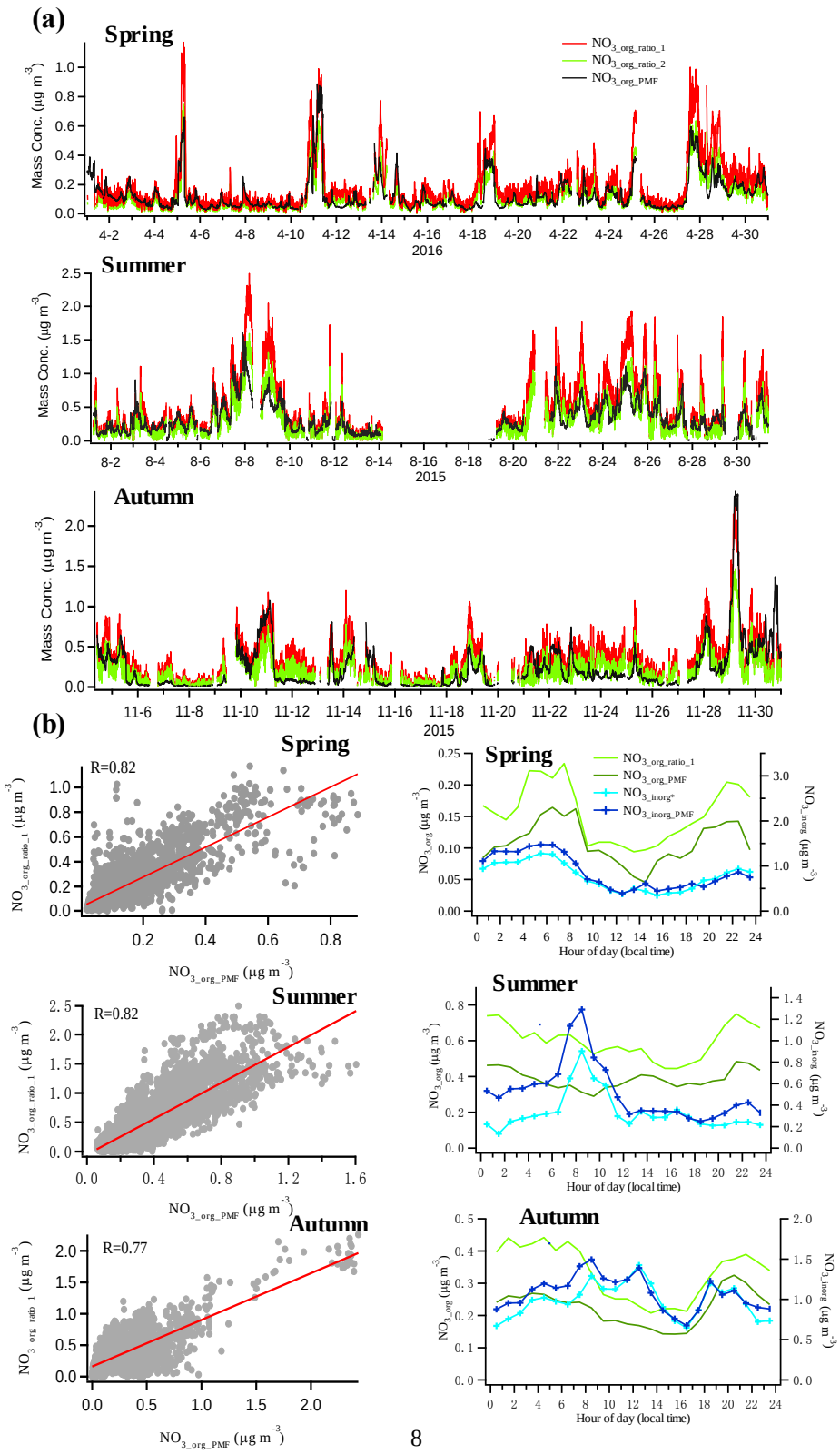
(a)
Spring
NO3_org_ratio_1
NO3_org_ratio_2
NO3_org_PMF
Mass Conc. (μg m-3)
2016
Summer
2015
Autumn
2015
(b)
Spring
R=0.82
NO3_org_ratio_1 (μg m-3)
NO3_org_PMF (μg m-3)
NO3_org_ratio_1
NO3_org_PMF
NO3_inorg*
NO3_inorg_PMF
NO3_org (μg m-3)
NO3_inorg (μg m-3)
Hour of day (local time)
Summer
R=0.82
Autumn
R=0.77

Figure 2. (a) Time series of $NO_{3,\ org}$ concentration estimated by the NO^+/NO_2^+ ratio method and PMF method for each season; (b) correlations between $NO_{3\_org\_ratio\_1}$ and $NO_{3\_org\_PMF}$ (left panel); diurnal trends of organic nitrates and $NO_{3,\ org}$ estimated by the different methods (right panel).

3.2 Correlation between organic nitrates and OA factors

As indicated by the results in the PMF method, the majority of organic nitrates were associated with LO-OOA in spring, summer and autumn in the urban atmosphere in Shenzhen, implying a dominant secondary origin of organic nitrates. To further confirm this relationship, we made the correlation analysis between organic nitrates estimated by the NO^+/NO_2^+ ratio method and the three factors resolved by the PMF analysis with only organic mass spectra in the three seasons. Generally, organic nitrates were found better-correlated with LO-OOA (R=0.69-0.77 in Figure 3) than with HOA and MO-OOA (R=0.03-0.69 in Figures S6-S8), which is consistent with the fact that the majority of organic nitrates were associated with LO-OOA in the PMF method. However, the moderate correlation between organic nitrates and HOA implied possibility of direct emissions of organic nitrates. Furthermore, we found a noticeably improved correlation between LO-OOA and organic nitrates at night (19:00-6:00) and a reduced correlation during the daytime (7:00-18:00) in Figure 3, especially in summer, implying that organic nitrates formation might be more closely related to secondary formation at night.

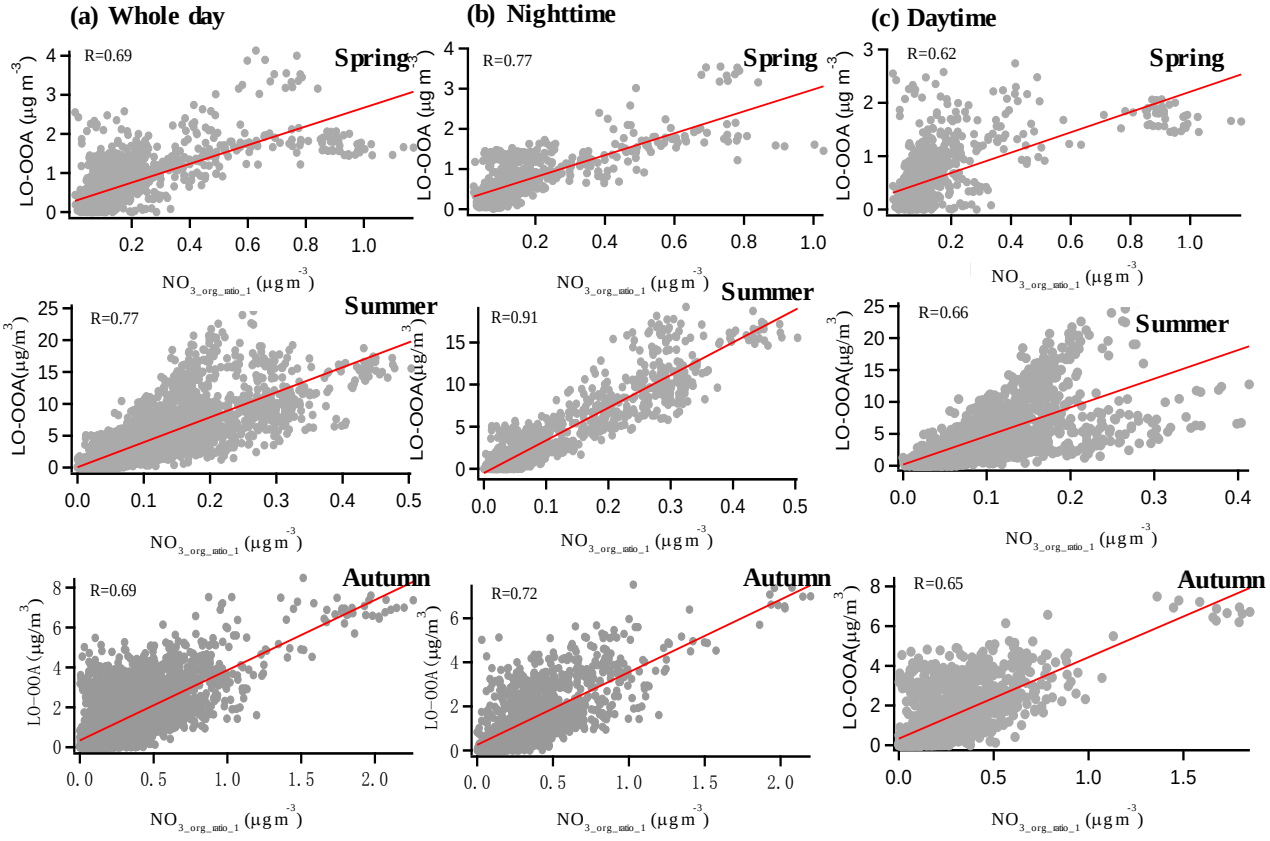

Figure 3. Correlation of $NO_{3\_org\_ratio\_1}$ and LO-OOA in each season for the whole day (a), at night (b) and in the daytime (c).

3.3 Size distribution characteristics of organic nitrates

In this section, we used the NO^+/NO_2^+ ratio as an indicator to investigate the size distribution of organic nitrates. The size distributions of the NO^+ and NO_2^+ signals for the different seasons have been shown in Figure S11. Due to the lack of HR-PToF data, our analyses used the UMR-PToF data (m/z 30 and 46), which may bring in the interferences of $CH_2O_X^+$. However, for all four seasons, the contributions of $CH_2O_X^+$ in m/z 30 and 46 in the HR data of PM_1 were less than 10% (Figure S10), which indicates that the interferences were negligible in this study. The average size distributions of different aerosol species and NO^+/NO_2^+ ratio in four seasons are shown in Figure 4a. It is clearly found that the NO^+/NO_2^+ ratio exhibited a decreasing trend in spring, summer and autumn, while it kept constant in winter, similar to the value of R_{NH4NO3} (red dotted line in Figure 4). It should also be noted that in spring, summer and autumn, the lowest values of NO^+/NO_2^+ ratio occurring at >1 μm approximated to the corresponding seasonal values of R_{NH4NO3}. These characteristics clearly indicated that organic nitrates existed mostly in fresh particles with smaller sizes. Different from the bulk OA and inorganic spices, very limited amount of organic nitrates exist in larger aged particles, implying that they could be easily removed by deposition and/or chemical degradation during air mass transport. In addition, the diurnal trends of size distribution of NO^+/NO_2^+ ratio in spring, summer and autumn in Figure 4b show apparent higher values at small sizes at night, suggesting an important nighttime local origin of organic nitrates. Combining with the analysis in section 3.2, local nighttime secondary formation of organic nitrates in warmer seasons in the urban polluted atmosphere in Shenzhen is highlighted. This is consistent with the previous findings in the US and Europe that the nighttime NO_3+VOCs reactions serve as an important source for particulate organic nitrates (Rollins et al., 2012; Xu et al., 2015a, 2015b; Fry et al., 2013; Lee et al., 2016). We will then explore the nighttime NO_3+VOCs reactions in Shenzhen in the following section.

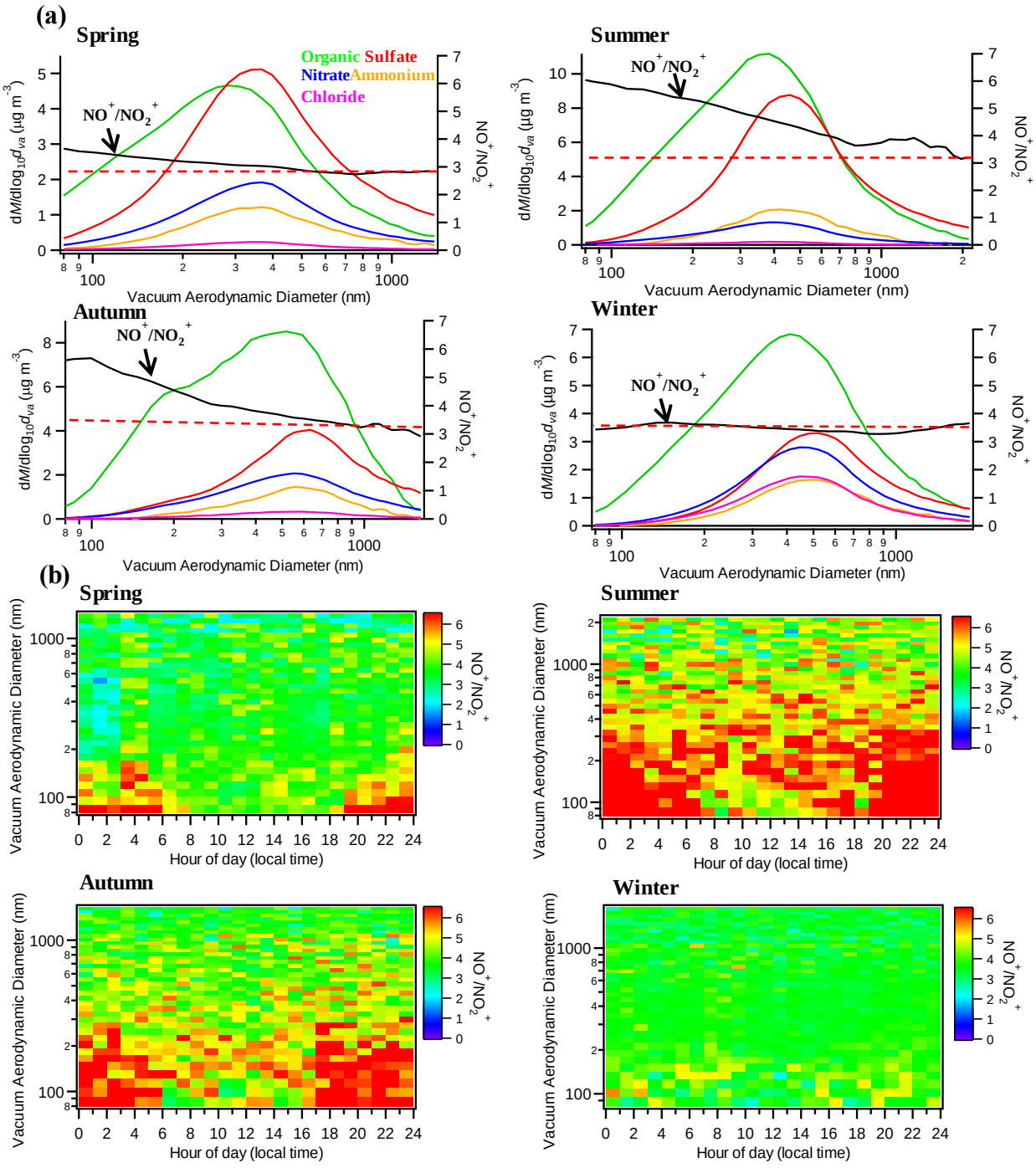

Figure 4.(a) Average size distributions of aerosol species and NO^+/NO_2^+ ratio (red dotted line represents R_{NH4NO3}); (b) diurnal trends of size distribution of NO^+/NO_2^+ ratio.

3.4 Nighttime particulate organic nitrates formation via NO_3+VOCs

Since on-line VOCs measurement was only performed during the spring campaign (described in section 2.2), the following theoretical analysis of NO_3+VOCs reactions applies only to the spring case. NO_3+VOCs reactions would yield a large mass of gas- and particle-phase organic nitrates (Rollins et al., 2012; Nah et al., 2016; Boyd et al., 2015, 2017; Xu et al., 2015a, 2015b; Lee et al., 2016). We used Eq. (9) to roughly judge the production potential (PP) of organic nitrates from a NO_3+VOC reaction:

$$[\text{Production Potential}]_{\text{NO3+VOCi}} = K_i \cdot [VOC_i] \cdot [NO_3] \quad (9)$$

Where K_i represents the reaction rate coefficient for NO_3 radical and a VOC; $[VOC_i]$ is the concentration of the specific VOC $[NO_3]$ is the concentration of NO_3 radical. It should be noted that no organic nitrates yield parameter was introduced in Eq. (9), because only a few organic nitrate yields for BVOCs were available in the literature (Fry et al., 2014; Ng et al., 2017). However, given the fact that the values of $K_i \cdot [VOC_i] \cdot [NO_3]$ for different VOC species can differ by orders of magnitude, not multiplying the organic nitrate yields (ranging from 0 to 1) would not significantly affect the PP ranking of VOCs. In the spring campaign, the diurnal variations of NO_2, O_3 and estimated NO_3 radical concentrations are shown in Figure S12. It was found that as a comparison to the nighttime NO_3 radical concentrations reported in literature in the United States (Rollins et al., 2012; Xu et al., 2015a), high concentrations of NO_2 (19.93±2.31 ppb) at night leaded to high yield of NO_3 radical (1.24±0.76 ppt) in Shenzhen, as calculated in Text S1.

The reaction rate coefficients of typical measured nighttime VOC concentrations with NO_3 radical and the production potentials are listed in Table S3 and shown in Figure 5. These VOCs were considered based on their higher ambient concentrations and availability for reaction kinetics with NO_3 radical. According to the distribution of production potential, five biogenic VOCs (BVOCs) (i.e., α-pinene, limonene, camphene, β-pinene and isoprene) and one anthropogenic VOC (styrene) were identified as notable VOC precursors with high production potential, while the sum of production potential from the other VOCs was negligible as shown in Figure 5b.

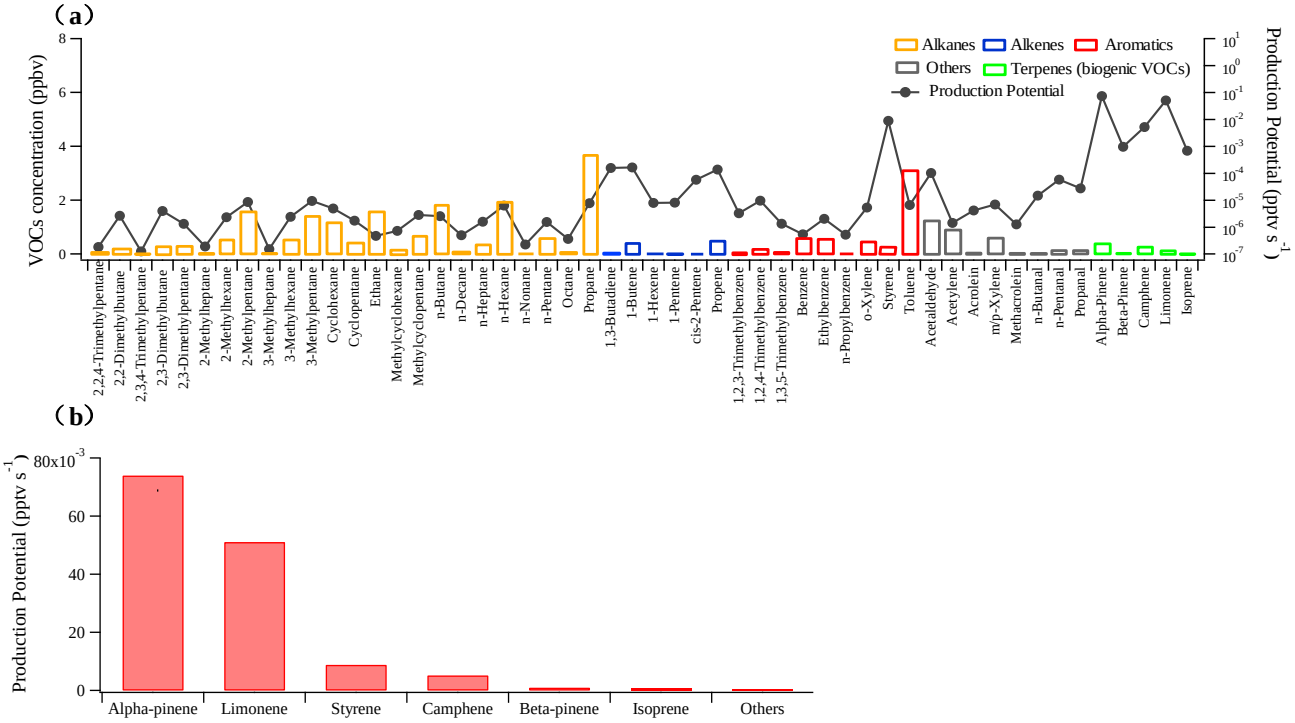

Figure 5. (a) Mean concentrations of VOCs and the corresponding calculated production potential of NO_3+VOC at night during the spring campaign; (b) production potential ranking of VOCs at night during the spring campaign.

Based on the production potential evaluation above, we further explore SOA yield of NO_3+the six notable VOC precursors according to the analysis method of particulate organic nitrate formation in Xu et al. (2015a). Briefly, NO_3 and ozone are two main oxidants for SOA formation from VOCs at night. Based on the concentrations of oxidants and the reaction rate constants for VOCs with NO_3 and ozone, the branching ratio of each VOC that reacts with NO_3 can be estimated as in Eq. (10). By combining the estimated branching ratios and SOA yields from chamber studies (Table 3), potential SOA production from these VOCs can be calculated as in Eq. (11) (Xu et al., 2015a):

$$branching\ ratio_{species\ i+NO3} = \frac{k_{[species\ i+NO3]} \times [NO_3]}{k_{[species\ i+NO3]} \times [NO_3] + k_{[species\ i+O3]} \times [O_3]} \quad (10)$$

$$[SOA]_{species,oxidant} = [species] \times branching\ ratio_{species,oxidant} \times yield_{species,\ oxidant} \quad (11)$$

The results in Table 3 show that all six notable VOC species were prone to react with NO_3 radical instead of O_3 at night, and the estimated potential SOA production from NO_3+VOCs reactions using SOA mass yields in the literature was 0-0.33 μg m^{-3} for α-pinene, 0.09-1.28 μg m^{-3} for limonene, 0.24 μg m^{-3} for styrene, 0.004-0.06 μg m^{-3} for β-pinene and 0.002-0.02 μg m^{-3} for isoprene. The SOA yield from camphene is currently unknown in the literature. It is seen that the average observed

nighttime concentration of particulate organic nitrates during the spring campaign (0.39-0.83μg m^{-3}, converting $NO_{3.org\_ratio\_1}$, $NO_{3.org\_PMF}$ in Figure 6 into organic nitrates assuming the average molecular weight of organic nitrates of 200 to 300 g mol^{-1}) was well within the estimated SOA concentration ranges produced by α-pinene, limonene and styrene in Table 3, indicating that these three VOCs were the key VOC precursors in urban atmosphere in Shenzhen. Considering both the production potentials and SOA yields, the contributions of β-pinene and isoprene to nighttime formation of particulate organic nitrates could be negligible.

Table 3. Average concentrations, reaction branching and SOA production of α-pinene, limonene, styrene, camphene, β-pinene and isoprene with respect to different oxidants at night in the spring campaign.

Species	Concentration (ppbv)	Rate coefficient [a]		Branching ratio		SOA yield from the literature (with NO_3)	SOA from VOCs + NO_3 ($\mu g\ m^{-3}$)
		NO_3	O_3	NO_3	O_3		
α-pinene	0.39	6.64E-12	7.2E-17	0.962	0.038	0-0.16[b]	0-0.33
Limonene	0.14	1.22E-11	1.54E-16	0.957	0.043	0.12-1.74[c]	0.09-1.28
Styrene	0.19	1.50E-12	1.70E-17	0.941	0.059	0.23[d]	0.24
Camphene	0.28	6.20E-13	9.0E-19	0.992	0.008	/	/
β-pinene	0.01	2.51E-12	1.50E-17	0.968	0.032	0.07-1.04[e]	0.004-0.06
Isoprene	0.032	6.96E-13	1.27E-17	0.908	0.091	0.02-0.24 [f]	0.002-0.02

[a] Rate coefficients for all species except camphene are from the Master Chemical Mechanism model (http://mcm.leeds.ac.uk/MCM/; under 25 ˚C), rate coefficients for camphene are from Martínez et al. (1999) and Atkinson et al. (1990).

[b] Hallquist et al. (1999); Spittler et al. (2006); Perraud et al. (2010); Fry et al. (2014); Nah et al. (2016).

[c] Fry et al. (2011, 2014); Spittler et al. (2006); Boyd et al. (2017).

[d] Cabrera-Perez et al. (2017).

[e] Griffin et al. (1999); Fry et al. (2009); Fry et al. (2014); Boyd et al. (2015).

[f] Rollins al. (2009); Ng et al. (2008).

The estimation of potential SOA production above suggests significant contributions of α-pinene, limonene, and styrene to SOA, and the significant contribution of camphene is also possible. Thus, we further explored the diurnal variations of the PPs of these four VOCs. Figure 6 shows the diurnal trends of BC, LO-OOA, $NO_{3.org\_ratio\_1}$, $NO_{3.org\_PMF}$, and the PPs of the four VOCs during the spring campaign. There were two apparent nighttime growth periods (i.e., I: 19:00–22:00 and II: 2:00–6:00) for both $NO_{3.org\_ratio\_1}$ and $NO_{3.org\_PMF}$. During Period I, BC maintained a relatively higher level, suggesting stable anthropogenic emissions. In contrast, the increases of all the PPs during Period I indicated that these precursors contributed to the organic nitrate growth. After 22:00, while the PPs still showed a rapid growth, BC and organic nitrates began to decrease, implying

possible existence of other important anthropogenic VOC precursors, which were not identified by the GC-FID/MS analysis but would dominate the formation of organic nitrates at this stage. During Period II, the anthropogenic emissions remained at a stable lower level, as indicated by BC, while all the PPs increased with organic nitrates again, indicating that these four precursors also contributed to, or could dominate, this organic nitrate growth. As shown in Figure S13, organic nitrates correlated better with the PPs (R=0.63–0.74) than with LO-OOA (R=0.19–0.31) or BC (R=0.02–0.05) during Period II at the spring campaign, suggesting the significant contributions of the NO_3 reactions with these precursors.

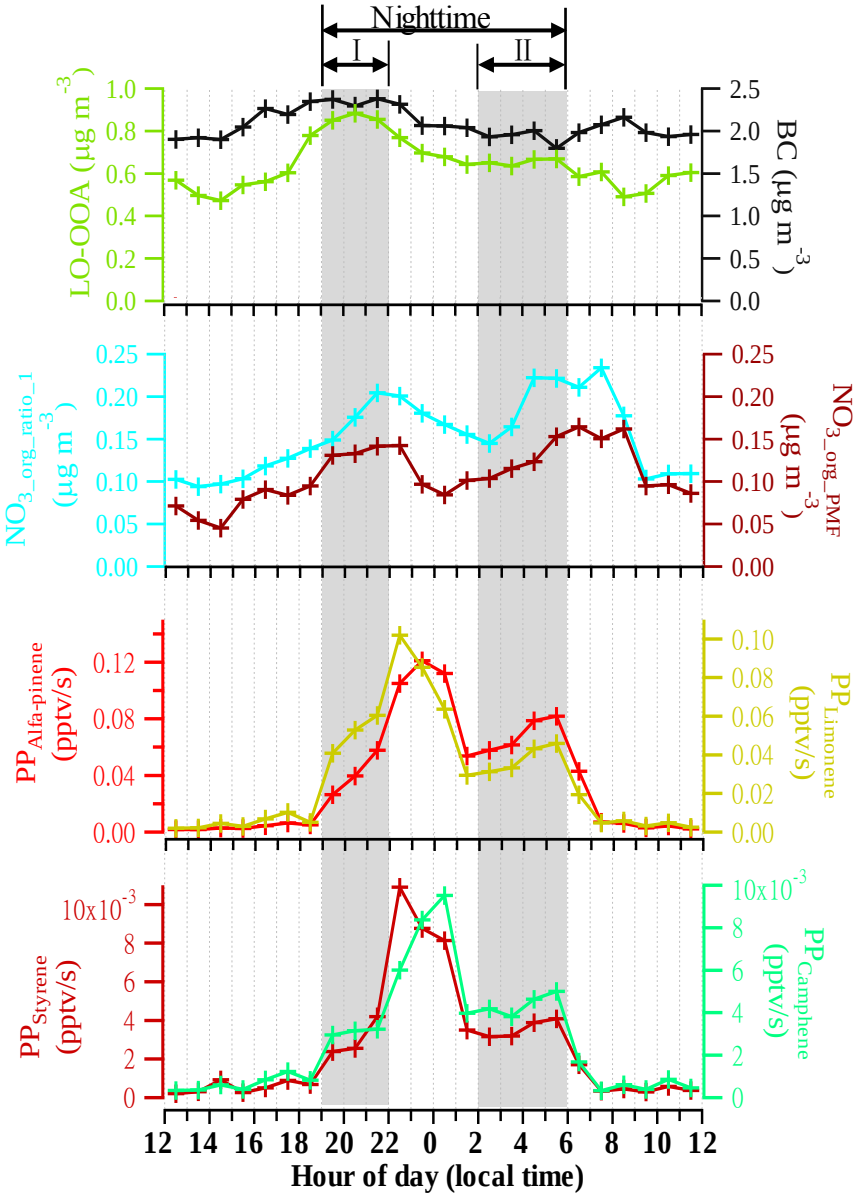

Figure 6. Diurnal trends of BC, LO-OOA, $NO_{3.org\_ratio\_1}$, $NO_{3.org\_PMF}$ and production potential (PP) of α-pinene, limonene, styrene, and camphene during the spring campaign.

It should be noted that, all previous studies on nighttime organic nitrate formation in the US and Europe focused on mechanisms of NO_3 reactions with BVOCs (Hallquist et al., 1999; Spittler et al., 2006; Perraud et al., 2010; Fry et al., 2014; Nah et al., 2016; Boyd et al., 2015, 2017). In this study, however, we found that anthropogenic VOCs could also play significant roles in particulate organic nitrate formation at night. Besides styrene, one of major aromatics (Cabrera-Perez et al., 2016), there were also other important anthropogenic VOC precursors that we did not identify in the spring campaign. In China, styrene has been actually identified as an important VOC of non-methane hydrocarbons (NMHCs) in urban areas, and has a notable contribution to ozone formation and SOA production (An et al., 2009; Yuan et al., 2013; Zhu et al., 2019). This study highlights the possible key roles of anthropogenic VOC precursors in nighttime particulate organic nitrate formation in urban atmosphere in China, and relevant smog chamber studies for anthropogenic VOCs+NO_3 reactions are needed to support parameterization in modeling.

3.5 Comparison with other similar studies and implications

Table 4 shows the average ambient temperatures, average concentrations of NO, NO_2, monoterpenes, $NO_{3,org}$, the ratio of $NO_{3,org}$ to $NO_{3,total}$ and the ratio of organic nitrates to total organics in several similar field campaigns available in the literature, which implies the key role of NO_3+VOCs reactions for nighttime particulate organic nitrate formation. In general, the variation of the particulate organic nitrates concentration is within an order of magnitude (0.06-0.98 $\mu g/m^3$) among the different sites. Higher concentrations of particulate organic nitrates generally is associate with higher NOx concentrations rather than BVOC concentrations. On the other hand, although the BVOC concentrations in Bakersfield were far less than that in other campaigns, the concentration of particulate organic nitrates there showed an intermediate level among all the campaigns. Therefore, it is suggested that the formation of particulate organic nitrates may be more relevant with NOx than BVOCs, which is consistent with the finding that the organic nitrate production was dominated by NOx in the southeastern US (Edwards et al., 2017). In the spring campaign of this study, we examined the correlation between organic nitrates and NO_2 or VOCs (by the sum of α-pinene, limonene, styrene and camphene) at night (Figure S14) and found a significant correlation of organic nitrates with NO_2 (R=0.40-0.47) rather than with VOCs (R=0.22-0.23), which further suggests that the organic nitrates formation was driven by the NOx-involved NO_3 chemistry.

313 **Table 4.** Average ambient temperatures, average concentrations of monoterpenes, $NO_{3,total}$, $NO_{3,org}$, $NO_{3,org}$/ $NO_{3,total}$ and the ratio of organic nitrates to total organics (ON/Org) for different
314 field campaigns around the world. The ON results at the European and US sites are from Kiendler-Scharr et al. (2016) and Ng et al. (2017).

Sampling site	**Site type**	**Sampling period**	**Temperature (°C)**	**NO (ppbv)**	**NO_2 (ppbv)**	**Monoterpenes (ppbv)**	**$NO_{3,org}$ (μg m^{-3})**	**$NO_{3,org}$/ $NO_{3,total}$**	**ON/Org**	**Reference/Note**
Bakersfield, **US**	rural	May-June, 2010	23.0		8.2	0.045 (α-pinene) 0.004 (β-pinene) 0.034 (limonene)	0.16	0.28	0.23	Rollins et al. (2012)/ NO3,org measured by TD-LIF
Woodland Park, **US**	high attitude	July-August, 2011	15.0		1.2	0.25 (monoterpene)	0.06	0.86	0.09	Fry et al. (2013)/ Use AMS data to estimate NO3,org
Centreville, **US**	rural	June-July, 2013	24.7	0.1	1.1	0.350 (α-pinene)* 0.312 (β-pinene)* 0.050 (limonene)*	0.08	1.00	0.10	Xu et al. (2015a) Xu et al. (2015b)/ Use AMS data to estimate NO3,org
Barcelona, **Spain**	urban	March, 2009	13.3	11.0	23.6	0.423 (monoterpene)	0.48	0.13	0.13	Mohr et al. (2012) Pandolfi et al. (2014) / Use AMS data to estimate NO3,org
Shenzhen, **China**	urban	April, 2016	24.5	8.0	19.4	0.391 (α-pinene)* 0.013 (β-pinene)* 0.137 (limonene)*	0.16	0.17	0.11	This study/ Use AMS data to estimate NO3,org

315 *BVOC concentration at night.

4. Conclusions

An Aerodyne HR-ToF-AMS was deployed in urban Shenzhen for about one month per season during 2015–2016 to characterize particulate organic nitrates with high time resolution. We discovered high mass fractions of organic nitrates in total organics during warmer seasons, including spring (9-21%), summer (11-25%) and autumn (9-20%), while particulate organic nitrates were negligible in winter. The correlation analysis between organic nitrates and each OA factor showed high correlation (R=0.77 in spring, 0.91 in summer and 0.72 in autumn) between organic nitrates and LO-OOA at night. The diurnal trend analysis of size distribution of NO^+/NO_2^+ ratio further suggested that organic nitrates formation mainly occurred at night. It also suggested that organic nitrates concentrated on smaller sizes, indicating that they were mostly local product. The calculated theoretical nighttime production potential of NO_3 reactions with VOCs measured in spring showed that six VOC species (i.e., α-pinene, limonene, styrene, camphene, β-pinene and isoprene) were prominent precursors. The SOA yield analysis and the nighttime variation of production potential further indicated that α-pinene, limonene, camphene and styrene could contribute significantly to nighttime formation of particulate organic nitrates in spring in Shenzhen, highlighting the unique contribution of anthropogenic VOCs as a comparison to that documented in previous studies in the US and Europe. Finally, the comparison of the results in this study with other similar studies implied that nighttime formation of particulate organic nitrates is more relevant with NOx levels.

Acknowledgments

This work was supported by National Key R&D Program of China (2018YFC0213901), National Natural Science Foundation of China (91544215; 41622304) and Science and Technology Plan of Shenzhen Municipality (JCYJ20170412150626172).

References

An, J. L., Wang, Y. S., Sun, Y.: Effects of nonmethane hydrocarbons on ozone formation in Beijing. Ecology & Environmental Sciences.

Atkinson, R., Aschmann, S. M., Arey, J.: Rate constants for the gas-phase reactions of OH and NO3 radicals and O3 with sabinene and camphene at 296±2 K. Atmospheric Environment. Part A. General Topics, 24, (10), 2647-2654, https://doi.org/10.1016/0960-1686(90)90144-C, 1990

Ayres, B.R., Allen, H.M., Draper, D.C., Brown, S.S., Wild, R.J., Jimenez, J.L., Day, D.A., Campuzano-Jost, P., Hu, W., De Gouw, J.A., Koss, A., Cohen, R.C., Duffey, K.C., Romer, P., Baumann, K., Edgerton, E., Takahama, S., Thornton, J.A., Lee, B.H., Lopez-Hilfiker, F.D., Mohr, C., Wennberg, P.O., Nguyen, T.B., Teng, A.P., Goldstein, A.H., Olson, K., Fry,

J.L.: Organic nitrate aerosol formation via NO3+ biogenic volatile organic compounds in the southeastern United States. Atmos. Chem. Phys. 15, 13377-13392. https://doi.org/10.5194/acp-15-13377-2015, 2015.

Boyd, C.M., Nah, T., Xu, L., Berkemeier, T., Ng, N.L.: Secondary Organic Aerosol (SOA) from Nitrate Radical Oxidation of Monoterpenes: Effects of Temperature, Dilution, and Humidity on Aerosol Formation, Mixing, and Evaporation. Environ. Sci. Technol. 51, 7831–7841. https://doi.org/10.1021/acs.est.7b01460, 2017.

Boyd, C.M., Sanchez, J., Xu, L., Eugene, A.J., Nah, T., Tuet, W.Y., Guzman, M.I., Ng, N.L.: Secondary organic aerosol formation from the β-pinene+NO3 system: effect of humidity and peroxy radical fate. Atmos. Chem. Phys. 15, 7497-7522. https://doi.org/10.5194/acp-15-7497-2015, 2015.

Bruns, E.A., Perraud, V., Zelenyuk, A., Ezell, M.J., Johnson, S.N., Yu, Y., Imre, D., Finlayson-Pitts, B.J., Alexander, M.L.: Comparison of FTIR and particle mass spectrometry for the measurement of particulate organic nitrates. Environ. Sci. Technol. 44, 1056-1061. https://doi.org/10.1021/es9029864, 2010.

Cabrera-Perez, D., Taraborrelli, D., Sander, R., and Pozzer, A.: Global atmospheric budget of simple monocyclic aromatic compounds, Atmos. Chem. Phys., 16, 6931-6947, https://doi.org/10.5194/acp-16-6931-2016, 2016.

Cabrera-Perez, D., Taraborrelli, D., Lelieveld, J., Hoffmann, T., and Pozzer, A.: Global impact of monocyclic aromatics on tropospheric composition, Atmos. Chem. Phys. Discuss., https://doi.org/10.5194/acp-2017-928, 2017.

Canagaratna, M.R., Jayne, J.T., Jimenez, J.L., Allan, J.D., Alfarra, M.R., Zhang, Q., Onasch, T.B., Drewnick, F., Coe, H., Middlebrook, A., Delia, A., Williams, L.R., Trimborn, A.M., Northway, M.J., DeCarlo, P.F., Kolb, C.E., Davidovits, P., Worsnop, D.R.: Chemical and microphysical characterization of ambient aerosols with the aerodyne aerosol mass spectrometer. Mass Spectrom. Rev. 26, 185-222. https://doi.org/10.1002/mas.20115, 2007.

Cubison, M. J., Ortega, A. M., Hayes, P. L., Farmer, D. K., Day, D., Lechner, M. J., Brune, W. H., Apel, E., Diskin, G. S., Fisher, J. A., Fuelberg, H. E., Hecobian, A., Knapp, D. J., Mikoviny, T., Riemer, D., Sachse, G. W., Sessions, W., Weber, R. J., Weinheimer, A. J., Wisthaler, A., and Jimenez, J. L.: Effects of aging on organic aerosol from open biomass burning smoke in aircraft and laboratory studies, Atmos. Chem. Phys., 11, 12049-12064, https://doi.org/10.5194/acp-11-12049-2011, 2011.

Day, D. A., Liu, S., Russell, L. M., and Ziemann, P. J.: Organonitrate group concentrations in submicron particles with high nitrate and organic fractions in coastal southern California, Atmos. Environ., 44, 1970–1979, https://doi.org/10.1016/j.atmosenv.2010.02.045, 2010.

DeCarlo, P.F., Kimmel, J.R., Trimborn, A., Northway, M.J., Jayne, J.T., Aiken, A.C., Gonin, M., Fuhrer, K., Horvath, T., Docherty, K.S., Worsnop, D.R., Jimenez, J.L.: Field-deployable, high-resolution, time-of-flight aerosol mass spectrometer. Anal. Chem. 78, 8281-8289. https://doi.org/10.1021/ac061249n, 2006.

Edwards, P. M.; Aikin, K. C.; Dube, W. P.; Fry, J. L.; Gilman, J. B.; de Gouw, J. A.; Graus, M. G.; Hanisco, T. F.; Holloway, J.; Hübler, G.; Kaiser, J.; Keutsch, F. N.; Lerner, B. M.; Neuman, J. A.; Parrish, D. D.; Peischl, J.; Pollack, I. B.; Ravishankara, A. R.; Roberts, J. M.; Ryerson, T. B.; Trainer, M.; Veres, P. R.; Wolfe, G. M.; Warneke, C.; Brown, S. S.:

Transition from high- to low-NOx control of night-time oxidation in the southeastern US. Nature Geoscienc, 10, (7), 490-495. https://doi.org/10.1038/ngeo2976, 2017.

Farmer, D.K., Matsunaga, A., Docherty, K.S., Surratt, J.D., Seinfeld, J.H., Ziemann, P.J., Jimenez, J.L.: Response of an aerosol mass spectrometer to organonitrates and organosulfates and implications for atmospheric chemistry. Proc. Natl. Acad. Sci. 107, 6670-6675. https://doi.org/10.1073/pnas.0912340107, 2010.

Fry, J.L., Draper, D.C., Barsanti, K.C., Smith, J.N., Ortega, J., Winkler, P.M., Lawler, M.J., Brown, S.S., Edwards, P.M., Cohen, R.C.: Secondary Organic Aerosol Formation and Organic Nitrate Yield from NO3 Oxidation of Biogenic Hydrocarbons. Environ. Sci. Technol. 48, 11944–11953. https://doi.org/10.1021/es502204x, 2014.

Fry, J.L., Draper, D.C., Zarzana, K.J., Campuzano-Jost, P., Day, D.A., Jimenez, J.L., Brown, S.S., Cohen, R.C., Kaser, L., Hansel, A., Cappellin, L., Karl, T., Hodzic Roux, A., Turnipseed, A., Cantrell, C., Lefer, B.L., Grossberg, N.: Observations of gas- and aerosol-phase organic nitrates at BEACHON-RoMBAS 2011. Atmos. Chem. Phys. 13, 8585-8605. https://doi.org/10.5194/acp-13-8585-2013, 2013.

Fry, J.L., Kiendler-Scharr, A., Rollins, A.W., Brauers, T., Brown, S.S., Dorn, H.P., Dubé, W.P., Fuchs, H., Mensah, A., Rohrer, F., Tillmann, R., Wahner, A., Wooldridge, P.J., Cohen, R. C.: SOA from limonene: Role of NO3 in its generation and degradation. Atmos. Chem. Phys. 11, 3879-3894. https://doi.org/10.5194/acp-11-3879-2011, 2011.

Fry, J.L., Kiendlerscharr, A., Rollins, A.W., Wooldridge, P.J., Brown, S.S., Fuchs, H., Dube, W.P., Mensah, A., Dal Maso, M., Tillmann, R.: Organic nitrate and secondary organic aerosol yield from NO 3 oxidation of β-pinene evaluated using a gas-phase kinetics/aerosol partitioning model. Atmos. Chem. Phys. 9, 1431–1449. https://doi.org/10.5194/acp-9-1431-2009, 2009.

Griffin, R. J., Cocker, D. R., III, Flagan, R. C., and Seinfeld, J. H.: Organic aerosol formation from the oxidation of biogenic hydrocarbons. J. Geophys. Res., 104, 3555–3567, https://doi.org/10.1029/1998jd100049, 1999.

Hallquist, M., Wängberg, I., Ljungström, E., Barnes, I., Becker, K.H.: Aerosol and product yields from NO3radical-initiated oxidation of selected monoterpenes. Environ. Sci. Technol. 33, 553-559. https://doi.org/10.1021/es980292s, 1999.

Hao, L.Q., Kortelainen, A., Romakkaniemi, S., Portin, H., Jaatinen, A., Leskinen, A., Komppula, M., Miettinen, P., Sueper, D., Pajunoja, A., Smith, J.N., Lehtinen, K.E.J., Worsnop, D.R., Laaksonen, A., Virtanen, A.: Atmospheric submicron aerosol composition and particulate organic nitrate formation in a boreal forestland-urban mixed region. Atmos. Chem. Phys. 14, 13483-13495. https://doi.org/10.5194/acp-14-13483-2014, 2014.

He, L.Y., Huang, X.F., Xue, L., Hu, M., Lin, Y., Zheng, J., Zhang, R., Zhang, Y.H.: Submicron aerosol analysis and organic source apportionment in an urban atmosphere in Pearl River Delta of China using high-resolution aerosol mass spectrometry. J. Geophys. Res. Atmos. 116, D12. https://doi.org/10.1029/2010JD014566, 2011.

Huang, X.F., He, L.Y., Hu, M., Canagaratna, M.R., Sun, Y., Zhang, Q., Zhu, T., Xue, L., Zeng, L.W., Liu, X.G., Zhang, Y.H., Jayne, J.T., Ng, N.L., Worsnop, D.R.: Highly time-resolved chemical characterization of atmospheric submicron particles during 2008 Beijing Olympic games using an aerodyne high-resolution aerosol mass spectrometer. Atmos. Chem. Phys. 10, 8933-8945. https://doi.org/10.5194/acp-10-8933-2010, 2010.

Huang, X.F., He, L.Y., Xue, L., Sun, T.L., Zeng, L.W., Gong, Z.H., Hu, M., Zhu, T.: Highly time-resolved chemical characterization of atmospheric fine particles during 2010 Shanghai World Expo. Atmos. Chem. Phys. 12, 4897-4907. https://doi.org/10.5194/acp-12-4897-2012, 2012.

Huang, X.F., Xue, L., Tian, X.D., Shao, W.W., Sun, T. Le, Gong, Z.H., Ju, W.W., Jiang, B., Hu, M., He, L.Y.: Highly time-resolved carbonaceous aerosol characterization in Yangtze River Delta of China: Composition, mixing state and secondary formation. Atmos. Environ. 64, 200-207. https://doi.org/10.1016/j.atmosenv.2012.09.059, 2013.

Jimenez, J. L., Jayne, J. T., Shi, Q., Kolb, C. E., Worsnop, D. R., Yourshaw, I., Seinfeld, J. H., Flagan, R. C., Zhang, X. F., Smith, K. A., Morris, J. W., and Davidovits, P.: Ambient aerosol sampling using the aerodyne aerosol mass spectrometer, J. Geophys. Res.-Atmos., 108, 447–457, https://doi.org/10.1029/2001JD001213, 2003.

Kiendler-Scharr, A., Mensah, A. A., Friese, E., Topping, D., Nemitz, E., Prevot, A. S. H., Äijälä, M., Allan, J., Canonaco, F., Canagaratna, M., Carbone, S., Crippa, M., Dall Osto, M., Day, D. A., De Carlo, P., Di Marco, C. F., Elbern, H., Eriksson, A., Freney, E., Hao, L., Herrmann, H., Hildebrandt, L., Hillamo, R., Jimenez, J. L., Laaksonen, A., McFiggans, G., Mohr, C., O'Dowd, C., Otjes, R., Ovadnevaite, J., Pandis, S. N., Poulain, L., Schlag, P., Sellegri, K., Swietlicki, E., Tiitta, P., Vermeulen, A., Wahner, A., Worsnop, D., and Wu, H. C.: Organic nitrates from night-time chemistry are ubiquitous in the European submicron aerosol, Geophys. Res. Lett., 43, 7735–7744, https://doi:10.1002/2016GL069239, 2016.

Lee, B.H., Mohr, C., Lopez-Hilfiker, F.D., Lutz, A., Hallquist, M., Lee, L., Romer, P., Cohen, R.C., Iyer, S., Kurten, T., Hu, W., Day, D.A., Campuzano-Jost, P., Jimenez, J.L., Xu, L., Ng, N.L., Guo, H., Weber, R.J., Wild, R.J., Brown, S.S., Koss, A., de Gouw, J., Olson, K., Goldstein, A.H., Seco, R., Kim, S., McAvey, K., Shepson, P.B., Starn, T., Baumann, K., Edgerton, E.S., Liu, J., Shilling, J.E., Miller, D.O., Brune, W., Schobesberger, S., D'Ambro, E.L., Thornton, J.A.: Highly functionalized organic nitrates in the southeast United States: Contribution to secondary organic aerosol and reactive nitrogen budgets. Proc. Natl. Acad. Sci. 113, 1516-1521. https://doi.org/10.1073/pnas.1508108113, 2016.

Lelieveld, J., Gromov, S., Pozzer, A., Taraborrelli, D.: Global tropospheric hydroxyl distribution, budget and reactivity. Atmos. Chem. Phys. 16, 12477-12493. https://doi.org/10.5194/acp-16-12477-2016, 2016.

Martínez, E.; Cabañas, B.; Aranda, A.; Martín, P.; Salgado, S.: Absolute Rate Coefficients for the Gas-Phase Reactions of NO3 Radical with a Series of Monoterpenes at T = 298 to 433 K. Journal of Atmospheric Chemistry, 33, (3), 265-282. https://doi.org/10.1023/A:1006178530211, 1999.

Middlebrook, A.M., Bahreini, R., Jimenez, J.L., Canagaratna, M.R.: Evaluation of composition-dependent collection efficiencies for the Aerodyne aerosol mass spectrometer using field data. Aerosol Sci. Technol. 46, 258-271. https://doi.org/10.1080/02786826.2011.620041, 2012.

Mohr, C., DeCarlo, P. F., Heringa, M. F., Chirico, R., Slowik, J. G., Richter, R., Reche, C., Alastuey, A., Querol, X., Seco, R., Peñuelas, J., Jiménez, J. L., Crippa, M., Zimmermann, R., Baltensperger, U., and Prévôt, A. S. H.: Identification and quantification of organic aerosol from cooking and other sources in Barcelona using aerosol mass spectrometer data, Atmos. Chem.Phys., 12, 1649–1665, https://doi.org/10.5194/acp-12-1649-2012, 2012.

Nah, T., McVay, R. C., Zhang, X., Boyd, C. M., Seinfeld, J. H., and Ng, N. L.: Influence of seed aerosol surface area and oxidation rate on vapor wall deposition and SOA mass yields: a case study with α-pinene ozonolysis, Atmos. Chem. Phys., 16, 9361–9379, https://doi.org/10.5194/acp-16-9361-2016, 2016.

Ng, N. L., Brown, S. S., Archibald, A. T., Atlas, E., Cohen, R. C., Crowley, J. N., Day, D. A., Donahue, N. M., Fry, J. L., Fuchs, H., Griffin, R. J., Guzman, M. I., Herrmann, H., Hodzic, A., Iinuma, Y., Jimenez, J. L., Kiendler-Scharr, A., Lee, B. H., Luecken, D. J., Mao, J., McLaren, R., Mutzel, A., Osthoff, H. D., Ouyang, B., Picquet-Varrault, B., Platt, U., Pye, H. O. T., Rudich, Y., Schwantes, R. H., Shiraiwa, M., Stutz, J., Thornton, J. A., Tilgner, A., Williams, B. J., and Zaveri, R. A.: Nitrate radicals and biogenic volatile organic compounds: oxidation, mechanisms, and organic aerosol, Atmos. Chem. Phys., 17, 2103-2162, https://doi.org/10.5194/acp-17-2103-2017, 2017.

Ng, N. L., Canagaratna, M. R., Zhang, Q., Jimenez, J. L., Tian, J., Ulbrich, I. M., Kroll, J. H., Docherty, K.S., Chhabra, P.S., Bahreini, R., Murphy, S.M., Seinfeld, J.H., Hildebrandt, L., Donahue, N.M., Decarlo, P.F., Lanz, V.A., Prévôt, A.S.H., Dinar, E., Rudich, Y., Worsnop, D.R.: Organic aerosol components observed in Northern Hemispheric datasets from Aerosol Mass Spectrometry. Atmos. Chem. Phys. 10, 4625-4641. https://doi.org/10.5194/acp-10-4625-2010, 2010.

Ng, N. L., Kwan, A. J., Surratt, J. D., Chan, A. W. H., Chhabra, P. S., Sorooshian, A., Pye, H. O. T., Crounse, J. D., Wennberg, P. O., Flagan, R. C., and Seinfeld, J. H.: Secondary organic aerosol (SOA) formation from reaction of isoprene with nitrate radicals (NO3), Atmos. Chem. Phys., 8, 4117–4140, https://doi.org/10.5194/acp-8-4117-2008, 2008.

Pandolfi, M.; Querol, X.; Alastuey, A.; Jimenez, J. L.; Jorba, O.; Day, D.; Ortega, A.; Cubison, M. J.; Comerón, A.; Sicard, M.; Mohr, C.; Prévôt, A. S. H.; Minguillón, M. C.; Pey, J.; Baldasano, J. M.; Burkhart, J. F.; Seco, R.; Peñuelas, J.; van Drooge, B. L.; Artiñano, B.; Di Marco, C.; Nemitz, E.; Schallhart, S.; Metzger, A.; Hansel, A.; Lorente, J.; Ng, S.; Jayne, J.; Szidat, S.: Effects of sources and meteorology on particulate matter in the Western Mediterranean Basin: An overview of the DAURE campaign. Journal of Geophysical Research: Atmospheres, 119, (8), 4978-5010. https://10.1002/2013JD021079, 2014.

Perraud, V., Bruns, E. A., Ezell, M. J., Johnson, S. N., Greaves, J.,and Finlayson-Pitts, B. J.: Identification of organic nitrates in the NO3 radical initiated oxidation of α-pinene by atmospheric pressure chemical ionization mass spectrometry, Environ. Sci. Technol., 44, 5887–5893. https://doi.org/10.1021/es1005658, 2010.

Rollins, A.W., Browne, E.C., Min, K.-E., Pusede, S.E., Wooldridge, P.J., Gentner, D.R., Goldstein, A.H., Liu, S., Day, D.A., Russell, L.M., Cohen, R.C.: Evidence for NOx Control over Nighttime SOA Formation. Science. 337, 1210-1212. https://doi.org/10.1126/science.1221520, 2012.

Rollins, A. W., Kiendler-Scharr, A., Fry, J. L., Brauers, T., Brown, S. S., Dorn, H.-P., Dubé, W. P., Fuchs, H., Mensah, A., Mentel, T. F., Rohrer, F., Tilmann, R., Wegener, R., Wooldridge, P. J., and Cohen, R. C.: Isoprene oxidation by nitrate radical: alkyl nitrate and secondary organic aerosol yields, tmos. Chem. Phys., 9, 6685–6703, https://doi.org/10.5194/acp-9-6685-2009, 2009.

Sato, K., Takami, A., Isozaki, T., Hikida, T., Shimono, A., Imamura, T.: Mass spectrometric study of secondary organic aerosol formed from the photo-oxidation of aromatic hydrocarbons. Atmos. Environ. 44, 1080-1087. https://doi.org/10.1016/j.atmosenv.2009.12.013, 2010.

Sobanski, N., Thieser, J., Schuladen, J., Sauvage, C., Song, W., Williams, J., Lelieveld, J., Crowley, J.N.: Day and night-time formation of organic nitrates at a forested mountain site in south-west Germany. Atmos. Chem. Phys. 17, 4115-4130. https://doi.org/10.5194/acp-17-4115-2017, 2017.

Spittler, M., Barnes, I., Bejan, I., Brockmann, K.J., Benter, T., Wirtz, K.: Reactions of NO3 radicals with limonene and α-pinene : Product and SOA formation. Atmos. Environ. 40, 116–127. https://doi.org/10.1016/j.atmosenv.2005.09.093, 2006.

Sun, Y., Zhang, Q., Schwab, J.J., Yang, T., Ng, N.L., Demerjian, K.L.: Factor analysis of combined organic and inorganic aerosol mass spectra from high resolution aerosol mass spectrometer measurements. Atmos. Chem. Phys. 12, 8537–8551. https://doi.org/10.5194/acp-12-8537-2012, 2012.

Teng, A.P., Crounse, J.D., Lee, L., St. Clair, J.M., Cohen, R.C., Wennberg, P.O.: Hydroxy nitrate production in the OH-initiated oxidation of alkenes. Atmos. Chem. Phys. 139, 5367-5377. https://doi.org/10.5194/acp-15-4297-2015, 2015.

Teng, A.P., Crounse, J.D., Wennberg, P.O.: Isoprene Peroxy Radical Dynamics. J. Am. Chem. Soc. 15, 4297-4316. https://doi.org/10.1021/jacs.6b12838, 2017.

Wang, H.; Lu, K.; Chen, X.; Zhu, Q.; Chen, Q.; Guo, S.; Jiang, M.; Li, X.; Shang, D.; Tan, Z.; Wu, Y.; Wu, Z.; Zou, Q.; Zheng, Y.; Zeng, L.; Zhu, T.; Hu, M.; Zhang, Y.: High N_2O_5 Concentrations Observed in Urban Beijing: Implications of a Large Nitrate Formation Pathway. Environmental Science & Technology Letters, 4, (10), 416-420. https://doi.10.1021/acs.estlett.7b00341, 2018.

Wang, M.; Zeng, L.; Lu, S.; Shao, M.; Liu, X.; Yu, X.; Chen, W.; Yuan, B.; Zhang, Q.; Hu, M.; Zhang, Z.: Development and validation of a cryogen-free automatic gas chromatograph system (GC-MS/FID) for online measurements of volatile organic compounds, 6, (23), 9424-9434. Analytical Methods, https://doi.10.1039/C4AY01855A, 2014.

Xu, L., Guo, H., Boyd, C.M., Klein, M., Bougiatioti, A., Cerully, K.M., Hite, J.R., Isaacman-VanWertz, G., Kreisberg, N.M., Knote, C., Olson, K., Koss, A., Goldstein, A.H., Hering, S. V., de Gouw, J., Baumann, K., Lee, S.-H., Nenes, A., Weber, R.J., Ng, N.L.: Effects of anthropogenic emissions on aerosol formation from isoprene and monoterpenes in the southeastern United States. Proc. Natl. Acad. Sci. 112, 37-42. https://doi.org/10.1073/pnas.1417609112, 2015a.

Xu, L., Suresh, S., Guo, H., Weber, R.J., Ng, N.L.: Aerosol characterization over the southeastern United States using high-resolution aerosol mass spectrometry: Spatial and seasonal variation of aerosol composition and sources with a focus on organic nitrates. Atmos. Chem. Phys. 15, 7307-7336. https://doi.org/10.5194/acp-15-7307-2015, 2015b.

Xu, W., Sun, Y., Wang, Q., Du, W., Zhao, J., Ge, X., Han, T., Zhang, Y., Zhou, W., Li, J., Fu, P., Wang, Z., Worsnop, D.R.: Seasonal Characterization of Organic Nitrogen in Atmospheric Aerosols Using High Resolution Aerosol Mass Spectrometry in Beijing, China. ACS Earth Sp. Chem. 1, 673–682. https://doi.org/10.1021/acsearthspacechem.7b00106, 2017.

Yan, C., Nie, W., Äijälä, M., Rissanen, M.P., Canagaratna, M.R., Massoli, P., Junninen, H., Jokinen, T., Sarnela, N., Häme, S.A.K., Schobesberger, S., Canonaco, F., Yao, L., Prévôt, A.S.H., Petäjä, T., Kulmala, M., Sipilä, M., Worsnop, D.R., Ehn, M.: Source characterization of highly oxidized multifunctional compounds in a boreal forest environment using positive matrix factorization. Atmos. Chem. Phys. 16, 12715-12731. https://doi.org/10.5194/acp-16-12715-2016, 2016.

Yuan, B., Hu, W. W., Shao, M., Wang, M., Chen, W. T., Lu, S. H., Zeng, L. M., and Hu, M.: VOC emissions, evolutions and contributions to SOA formation at a receptor site in eastern China, Atmos. Chem. Phys., 13, 8815-8832, https://doi.org/10.5194/acp-13-8815-2013,2013.

Zhang, Q., Jimenez, J.L., Canagaratna, M.R., Ulbrich, I.M., Ng, N.L., Worsnop, D.R., Sun, Y.: Understanding atmospheric organic aerosols via factor analysis of aerosol mass spectrometry: A review. Anal. Bioanal. Chem. 401, 3045-3067. https://doi.org/10.1007/s00216-011-5355-y, 2011.

Zhang, Y.H., Su, H., Zhong, L.J., Cheng, Y.F., Zeng, L.M., Wang, X.S., Xiang, Y.R., Wang, J.L., Gao, D.F., Shao, M., Fan, S.J., Liu, S.C.: Regional ozone pollution and observation-based approach for analyzing ozone-precursor relationship during the PRIDE-PRD2004 campaign. Atmos. Environ. 42, 6203-6218. https://doi.org/10.1016/j.atmosenv.2008.05.002, 2008.

Zhu, B., Han, Y., Wang, C., Huang, X. F., Xia, S. Y., Niu, Y. B., Yin, Z. X, He, L.Y. :Understanding primary and secondary sources of ambient oxygenated volatile organic compounds in Shenzhen utilizing photochemical age-based parameterization method. Journal of Environmental Sciences, 75, 105-114. https://doi.org/10.1016/j.jes.2018.03.008, 2019.

Zhu, Q., He, L.Y., Huang, X.F., Cao, L.M., Gong, Z.H., Wang, C., Zhuang, X., Hu, M.: Atmospheric aerosol compositions and sources at two national background sites in northern and southern China. Atmos. Chem. Phys. 16, 10283-10297. https://doi.org/10.5194/acp-16-10283-2016, 2016.

Zhu, Q., Huang, X.-F., Cao, L.-M., Wei, L.-T., Zhang, B., He, L.-Y., Elser, M., Canonaco, F., Slowik, J. G., Bozzetti, C., El-Haddad, I., and Prévôt, A. S. H.: Improved source apportionment of organic aerosols in complex urban air pollution using the multilinear engine (ME-2), Atmos. Meas. Tech., 11, 1049-1060. https://doi.org/10.5194/amt-11-1049-2018, 2018.